

⁶³Extraction of χ from a measure of the area under the resonance line, as is sometimes done, is not feasible for very high accuracy measurements such as those reported here. The usual analysis connecting the area and χ is not necessarily valid for the case of He³, where practical running conditions give line shapes that deviate significantly from Lorentzian, and contain large contributions of free precession signal (see Sec. II D). In addition, most spectrometers will have nonlinearities amounting to at least a percent or so over the range of resonance-line voltage detected, and these nonlinearities would be difficult to account for in measuring the area under the line.

⁶⁴B. A. Jacobsohn and R. K. Wangsness, *Phys. Rev.* **73**, 942 (1948).

⁶⁵M. R. Gabillard, *C.R. Soc. Biol. (Paris)* **232**, 96 (1951).

⁶⁶That T_2 may have a small temperature dependence poses no problem, since $I''(t')$ is found to be only very weakly dependent upon T_2 . Calculation showed that for a change of T_2 from 30 to 250 msec (the range of T_2 's for our samples) $I''(t')$ changed only about 5%. The height of the experimental

resonance line where $\chi' = 0$, when corrected for changes in filling factor, was also observed to change only 5% over this range of T_2 's. Since T_2 is known to be constant to about $\pm 5\%$ or better in the data-collecting temperature regions of our experiments (Refs. 24 and 27), changes in T_2 could only give spurious line-height changes of less than 0.04%.

⁶⁷K. A. Kermach and J. B. S. Haldane, *Biometrika* **37**, 30 (1950).

⁶⁸E. R. Grilly and R. L. Mills, *Ann. Phys. (N.Y.)* **8**, 1 (1959); R. L. Mills, E. R. Grilly, and S. G. Sydorak, *Ann. Phys. (N.Y.)* **12**, 41 (1961).

⁶⁹W. J. Mullin, *Phys. Rev. Lett.* **20**, 254 (1968).

⁷⁰T. P. Bernat, Ph.D. thesis (Brandeis University, 1972) (unpublished).

⁷¹Y. Beers, *Introduction to the Theory of Error* (Addison-Wesley, Reading, Mass., 1957).

⁷²P. R. Benington, *Data Reduction and Error Analysis for the Physical Sciences* (McGraw-Hill, New York, 1969).

Solid-Solid and Solid-Fluid Phase Transitions in Terms of the Lattice Model

Tsuyoshi Horiguchi and Tomoyasu Tanaka*

Department of Physics, Ohio University, Athens, Ohio 45701

(Received 31 August 1972)

The order-disorder theory of a classical lattice model is used to obtain both the solid-solid phase transition and fluid-solid phase transition in a single system. In this model, the range of the interatomic potential is extended up to the fourth-neighbor distance. If the potential is suitably chosen, it is shown that the phase transitions between the bcc solid and fcc solid, between the bcc solid and fluid, and between the fcc solid and fluid occur within the Bragg-Williams approximation. The results are shown by the phase diagrams.

I. INTRODUCTION

Since Lennard-Jones and Devonshire¹ (LJD) formulated a theory of melting of solids in terms of the lattice model, the lattice model has been used by many authors in order to investigate theoretically the phase transition between the solid and fluid.^{2,3} A satisfactory explanation at least in the first approximation, has been given for the change of phase from the solid to the fluid in terms of the interatomic forces.

Recently, LJD theory has been refined and extended by Yoshida and Okamoto⁴ to explain the melting curve maximum, which is a fascinating phenomenon found at high pressures. (This must be distinguished from the critical temperature for the coexistence of solid and liquid. The melting curve maximum implies that it is not possible to transform solid phase continuously into liquid phase, in contrast with the case between liquid phase and gas phase.) In their theory, like in LJD theory, the ratio of the number of occupied lattice points to that of unoccupied lattice points is fixed and hence the volume change of the system is represented by the change in the lattice constant. By using an ef-

fective interatomic potential, the repulsive part of which is properly soft, and using the Bragg-Williams approximation, they obtained a melting curve which has a maximum in T - P phase diagram.

In high-pressure experiments,⁵⁻¹⁰ not only the melting curve maximum but also solid-solid phase transitions have been observed in several substances. It is now a well-established fact that some substances, e.g., Ce, Cs, and so on, undergo polymorphic transitions which contain several structural and also isostructural transitions. In some cases of isostructural transition, the mechanism is known to be the electronic transition, that is, the promotion of electrons from one shell to another or the collapse of one electron shell to another. The mechanism of some structural transitions is known to be the rearrangement of atoms from one structure to another. This may be due partly to the change in the mechanism of cohesion resulting from the electronic transition, but mostly to statistical effects. The typical example of the structural and isostructural transition is observed in the phase diagram of cesium,^{6,8} which is shown in Fig. 1. The two separate experimental results are superposed in one figure. The experi-

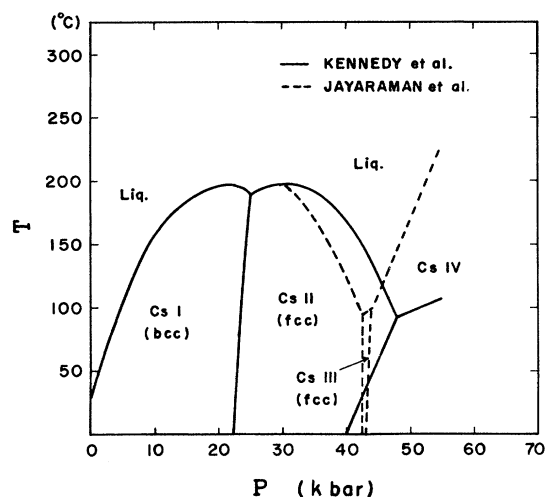


FIG. 1. T - P phase diagram for cesium. Solid line is given in Ref. 6. Dashed line is given in Ref. 8.

mental measurements do not seem to agree with each other especially in the high-pressure region. The first transition, the transition from phase I to phase II, was noted by Bardeen¹¹ to be the one in which cesium atoms were rearranged from bcc to fcc. The second one, from phase II to phase III, was suggested by Fermi¹² that the transition may represent an electron collapse of the 6s electron to the 5d state. Some theoretical calculations supported this mechanism. By x-ray diffraction studies, the crystal structures of Cs II and Cs III have been confirmed as fcc structure. However, it is not yet known whether the third one, from III to IV, is structural or isostructural.⁸

Some attempts have recently been made to study the isostructural transition.^{13,14} However, to the knowledge of the present authors, there is no statistical theory which explains the possibility of three-phase transitions, that is, structural solid-solid transition and solid-fluid transitions in a single system within the same theoretical framework. Since the structural transition is considered to be due mostly to statistical effect, we focus our attention to the transition near the triple point caused by the rearrangement of atoms like the first one in the phase diagram of Cs.

The purpose of this paper is to investigate the structural transition as well as solid-fluid transition in terms of the lattice model, and clarify what is essentially important in order to account for the solid-solid transition and high-pressure remelting. Our calculation is based on the simplified model in which the lattice constant is assumed to be unchangeable. In our model, the effect of diffusive motions of atoms is considered to be given by the migration of atoms from one lattice site to another, but the vibrational motions are completely neglected in

spite of their important role in the solid phase. In this paper we use the crudest approximation, i. e., the single-site approximation in the cluster-variation method,¹⁵ which is equivalent to the Bragg-Williams approximation. Thus, the short-range order is ignored, which is important not only in the liquid state but also in the region of the solid state near the melting temperature. One may, further, realize the fact that in real systems, like Cs, the interatomic distance does not change appreciably on phase transition from bcc to fcc structures, while in the present theory it changes from $\sqrt{3}$ to $\sqrt{2}$ in units of the simple cube-edge length, as will be described in Sec. II. Therefore, any detailed quantitative comparison of the present theory with experimental values would be insignificant. In Sec. II, the formulation is described within the single-site approximation using the cluster-variation method. In Sec. III, the results obtained by numerical calculation are shown in graphs with discussion. Concluding remarks are given in Sec. IV.

II. MODEL AND FORMULATION

It is most convenient to use the simple-cubic lattice as our basic lattice because it contains the bcc lattice and fcc lattice as its sublattices. By following LJD theory, we introduce the so-called normal and abnormal sites. All the lattice sites which belong to the sublattice constituting the desired lattice structure are called normal or α sites, and the remaining sites, belonging to the other sublattice, are called abnormal or β sites. The solid state, which is an ordered state, is characterized by having α sites more abundantly populated by atoms than β sites, and the fluid state, which is a disordered state, has all the lattice sites equally populated. As shown in Figs. 2(a) and 2(b), two different definitions of the normal and abnormal sites are considered. In Fig. 2(a), the ratio of the number of α sites to that of β sites is $\frac{1}{4}$, and the lattice structure of the solid phase is bcc. On the other hand, in Fig. 2(b), the number of α sites is equal to that of β sites, and the lattice structure of the solid is fcc.

The system we consider is a lattice gas in which N atoms are distributed over the L lattice sites of the basic simple cubic lattice with a lattice constant a . Then the number density is defined by

$$\rho = N/L = 1/v, \quad (2.1)$$

where $v = V/Na^3$ and $V = La^3$. The interatomic potential is assumed to be described by two-body central forces. In our calculation, the range of the interatomic potential is assumed to go up to the fourth-neighbor distance. It would be worthwhile to point out that this assumption is quite essential not because the range of the interatomic potential is long but because of our refinement of the lattice

model.

We shall first consider the case given by Fig. 2(a). Denoting the number densities of α sites and β sites by $\rho_{b\alpha}$ and $\rho_{b\beta}$, we have

$$\rho_{b\alpha} = N_{b\alpha} / L_{b\alpha}, \quad (2.2)$$

$$\rho_{b\beta} = N_{b\beta} / L_{b\beta}, \quad (2.3)$$

where $L_{b\alpha}$ and $L_{b\beta}$ are the number of the α sites and the number of β sites, respectively, and $N_{b\alpha}$ and $N_{b\beta}$ are the number of atoms on the α sites and the number of atoms on the β sites. We have the following relations:

$$N_{b\alpha} + N_{b\beta} = N, \quad (2.4)$$

$$L_{b\alpha} + L_{b\beta} = L, \quad (2.5)$$

$$L_{b\alpha} = \frac{1}{4}L. \quad (2.6)$$

The long-range order parameter is defined as

$$R_b = (\rho_{b\alpha} - \rho) / (1 - \rho). \quad (2.7)$$

As the completely ordered state is defined as the

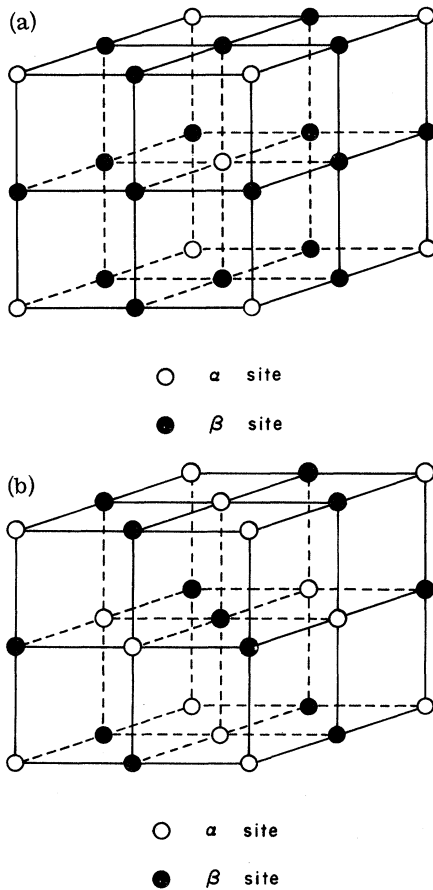


FIG. 2. (a) Simple cubic lattice which contains the bcc lattice as an α site. (b) Simple cubic lattice which contains the fcc lattice as an α site.

state in which all α sites are occupied, $\rho_{b\alpha}$ is equal to 1 and hence we have $R_b = 1$. In the completely disordered state the atoms are equally populated on both α and β sites; then $\rho_{b\alpha} = \rho$ and we have $R_b = 0$. The number densities on the α and β sites are expressed in terms of the long-range order parameter R_b , that is,

$$\rho_{b\alpha} = \rho + R_b(1 - \rho), \quad (2.8)$$

$$\rho_{b\beta} = \rho - \frac{1}{3}R_b(1 - \rho). \quad (2.9)$$

By using the lowest approximation of the cluster-variation method,¹⁵ which is equivalent to the Bragg-Williams approximation, the free energy per lattice site is given by

$$\begin{aligned} F_b/L = & \frac{1}{8} [z_3 \phi(r_3) + z_4 \phi(r_4)] \rho_{b\alpha}^2 \\ & + \frac{1}{4} [z_1 \phi(r_1) + z_2 \phi(r_2)] \rho_{b\alpha} \rho_{b\beta} \\ & + \frac{3}{8} [(z_1 - 2)\phi(r_1) + (z_2 - 4)\phi(r_2) \\ & + z_3 \phi(r_3) + z_4 \phi(r_4)] \rho_{b\beta}^2 \\ & + \frac{1}{4} kT [\rho_{b\alpha} \ln \rho_{b\alpha} + (1 - \rho_{b\alpha}) \ln(1 - \rho_{b\alpha}) \\ & + 3\rho_{b\beta} \ln \rho_{b\beta} + 3(1 - \rho_{b\beta}) \ln(1 - \rho_{b\beta})], \quad (2.10) \end{aligned}$$

where r_1 , r_2 , r_3 , and r_4 are the first-, second-, third-, and fourth-neighbor distances equal to a , $\sqrt{2}a$, $\sqrt{3}a$, and $2a$, respectively, and z_1 , z_2 , z_3 , and z_4 are the numbers of the first-, second-, third-, and fourth-neighbor lattice sites equal to 6, 12, 8, and 6, respectively. The potential energy is denoted by $\phi(r)$. k is the Boltzmann constant and T represents the temperature. By inserting Eqs. (2.8) and (2.9) into (2.10), one has

$$\begin{aligned} F_b/L = & [3\phi(r_1) + 6\phi(r_2) + 4\phi(r_3) + 3\phi(r_4)] \rho^2 \\ & - \frac{1}{3} [\phi(r_1) + 2\phi(r_2) - 4\phi(r_3) - 3\phi(r_4)] (1 - \rho)^2 R_b^2 \\ & + \frac{1}{4} kT \{ [\rho + (1 - \rho)R_b] \ln [\rho + (1 - \rho)R_b] \\ & + (1 - \rho)(1 - R_b) \ln [(1 - \rho)(1 - R_b)] \\ & + 3[\rho - \frac{1}{3}(1 - \rho)R_b] \ln [\rho - \frac{1}{3}(1 - \rho)R_b] \\ & + 3(1 - \rho)(1 + \frac{1}{3}R_b) \ln [(1 - \rho)(1 + \frac{1}{3}R_b)] \}. \quad (2.11) \end{aligned}$$

In the case of Fig. 2(b), Eqs. (2.2)–(2.5), (2.7), and (2.8) remain valid if $\rho_{f\alpha}$, $\rho_{f\beta}$, $N_{f\alpha}$, $N_{f\beta}$, $L_{f\alpha}$, $L_{f\beta}$, and R_f are substituted in place of $\rho_{b\alpha}$, $\rho_{b\beta}$, $N_{b\alpha}$, $N_{b\beta}$, $L_{b\alpha}$, $L_{b\beta}$, and R_b . Equations (2.6) and (2.9) are replaced by

$$L_f = \frac{1}{2}L, \quad (2.6')$$

$$\rho_{f\beta} = \rho - R_f(1 - \rho). \quad (2.9')$$

Within the same approximation as in Eq. (3.11), the free energy is expressed as

$$F_f/L = [3\phi(r_1) + 6\phi(r_2) + 4\phi(r_3) + 3\phi(r_4)] \rho^2$$

$$\begin{aligned}
& - [3\phi(r_1) - 6\phi(r_2) + 4\phi(r_3) - 3\phi(r_4)] (1 - \rho)^2 R_f^2 \\
& + \frac{1}{2} kT \{ [\rho + (1 - \rho)R_f] \ln[\rho + (1 - \rho)R_f] \\
& + (1 - \rho)(1 - R_f) \ln[(1 - \rho)(1 - R_f)] \\
& + [\rho - (1 - \rho)R_f] \ln[\rho - (1 - \rho)R_f] \\
& + (1 - \rho)(1 + R_f) \ln[(1 - \rho)(1 + R_f)] \}. \quad (2.12)
\end{aligned}$$

In the case of the disordered state corresponding to the fluid state, the two expressions for the free energy give the same result, i. e.,

$$\begin{aligned}
F_d/L = [3\phi(r_1) + 6\phi(r_2) + 4\phi(r_3) + 3\phi(r_4)] \rho^2 \\
+ kT [\rho \ln \rho + (1 - \rho) \ln(1 - \rho)]. \quad (2.13)
\end{aligned}$$

By minimizing the free energy F_b or F_f with respect to R_b or R_f , one obtains the minimum free energy F_b^{\min} and F_f^{\min} , and the corresponding long-range order parameters R_b and R_f . The true free energy of our system is considered to be given by

$$F = \text{Min}\{F_b^{\min}, F_f^{\min}, F_d\}. \quad (2.14)$$

Here F_b^{\min} or F_f^{\min} with zero-order parameter is equal to F_d . If F is equal to F_b^{\min} with nonzero R_b , to F_f^{\min} with nonzero R_f , or to F_d , our system will be either the bcc solid state, fcc solid state, or fluid state, respectively. Here, however, one must take the Maxwell construction into account in order to obtain the coexistence phase.

From the thermodynamic relations, we have

$$PV = -F + N \left(\frac{\partial F}{\partial N} \right)_{T,L}. \quad (2.15)$$

In our system, this equation is expressed as

$$Pa^3 = \frac{-F}{L} + \rho \left(\frac{\partial(F/L)}{\partial \rho} \right)_{T,L}. \quad (2.16)$$

By Eqs. (2.11)–(2.13), we have for the pressure of the bcc solid state, fcc solid state, and fluid state

$$\begin{aligned}
P_b a^3 = [3\phi(r_1) + 6\phi(r_2) + 4\phi(r_3) + 3\phi(r_4)] \rho^2 + \frac{1}{3} [\phi(r_1) + 2\phi(r_2) - 4\phi(r_3) - 3\phi(r_4)] (1 - \rho^2) R_b^2 \\
- \frac{1}{4} kT \{ R_b \ln[\rho + (1 - \rho)R_b] + (1 - R_b) \ln[(1 - \rho)(1 - R_b)] \\
- R_b \ln[\rho - \frac{1}{3}(1 - \rho)R_b] + (3 + R_b) \ln[(1 - \rho)(1 + \frac{1}{3}R_b)] \}, \quad (2.17)
\end{aligned}$$

$$\begin{aligned}
P_f a^3 = [3\phi(r_1) + 6\phi(r_2) + 4\phi(r_3) + 3\phi(r_4)] \rho^2 + [3\phi(r_1) - 6\phi(r_2) + 4\phi(r_3) - 3\phi(r_4)] (1 - \rho^2) R_f^2 \\
- \frac{1}{2} kT \{ R_f \ln[\rho + (1 - \rho)R_f] + (1 - R_f) \ln[(1 - \rho)(1 - R_f)] \\
- R_f \ln[\rho - (1 - \rho)R_f] + (1 + R_f) \ln[(1 - \rho)(1 + R_f)] \}, \quad (2.18)
\end{aligned}$$

$$P_d a^3 = [3\phi(r_1) + 6\phi(r_2) + 4\phi(r_3) + 3\phi(r_4)] \rho^2 - T \ln(1 - \rho). \quad (2.19)$$

By using the formula

$$\mu = \left(\frac{\partial(F/L)}{\partial \rho} \right)_{T,L}, \quad (2.20)$$

the expressions for the chemical potential of the bcc solid state, fcc solid state, and fluid state are given as

$$\begin{aligned}
\mu_b = 2[3\phi(r_1) + 6\phi(r_2) + 4\phi(r_3) + 3\phi(r_4)] \rho + \frac{2}{3} [\phi(r_1) + 2\phi(r_2) - 4\phi(r_3) - 3\phi(r_4)] (1 - \rho) R_b^2 \\
+ \frac{1}{4} kT \{ (1 - R_b) \ln[\rho + (1 - \rho)R_b] - (1 - R_b) \ln[(1 - \rho)(1 - R_b)] \\
+ (3 + R_b) \ln[\rho - \frac{1}{3}(1 - \rho)R_b] - (3 + R_b) \ln[(1 - \rho)(1 + \frac{1}{3}R_b)] \}, \quad (2.21)
\end{aligned}$$

$$\begin{aligned}
\mu_f = 2[3\phi(r_1) + 6\phi(r_2) + 4\phi(r_3) + 3\phi(r_4)] \rho + 2[3\phi(r_1) - 6\phi(r_2) + 4\phi(r_3) + 3\phi(r_4)] (1 - \rho) R_f^2 \\
+ \frac{1}{2} kT \{ (1 - R_f) \ln[\rho + (1 - \rho)R_f] - (1 - R_f) \ln[(1 - \rho)(1 - R_f)] \\
+ (1 + R_f) \ln[\rho - (1 - \rho)R_f] - (1 + R_f) \ln[(1 - \rho)(1 + R_f)] \}, \quad (2.22)
\end{aligned}$$

$$\mu_d = 2[3\phi(r_1) + 6\phi(r_2) + 4\phi(r_3) + 3\phi(r_4)] \rho + kT [\ln \rho - \ln(1 - \rho)]. \quad (2.23)$$

III. PHASE DIAGRAM

By using the formulation obtained in Sec. III, we shall discuss the phase transitions between the bcc solid and fcc solid, the bcc solid and fluid, and the fcc solid and fluid. We investigate the system de-

scribed by the Lennard-Jones potential

$$\phi(r) = 4\epsilon [(\sigma/r)^{12} - (\sigma/r)^6], \quad (3.1)$$

or by the exponential-type potential

$$\phi(r) = \epsilon \frac{\sigma^2 - r^2}{r_0^2 - \sigma^2} \exp\left(-\frac{r^2 - r_0^2}{r_0^2 - \sigma^2}\right). \quad (3.2)$$

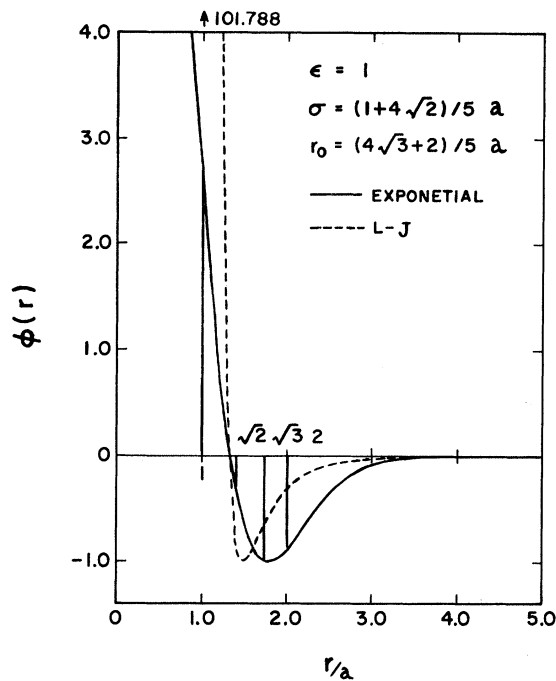


FIG. 3. Graph for the interatomic potential.

In Eqs. (3.1) and (3.2), σ is equal to the distance where the potential is equal to zero and $-\epsilon$ is equal to the minimum value of the potential. r_0 in Eq. (3.2) is the distance at which the potential has its minimum value $-\epsilon$. It is convenient to introduce the reduced temperature \tilde{T} , pressure \tilde{P} , free energy \tilde{F} , and chemical potential $\tilde{\mu}$, which are di-

mensionless quantities and defined by

$$\tilde{T} = kT/\epsilon, \quad (3.3)$$

$$\tilde{P} = Pa^3/\epsilon, \quad (3.4)$$

$$\tilde{F} = F/\epsilon, \quad (3.5)$$

$$\tilde{\mu} = \mu/\epsilon, \quad (3.6)$$

in terms of the parameter ϵ . In Fig. 3, the typical curves of the potential are shown for the Lennard-Jones potential with $\sigma/a = \frac{1}{5}(1+4\sqrt{2})$ and for the exponential-type potential with $\sigma/a = \frac{1}{5}(1+4\sqrt{2})$ and $r_0/a = \frac{1}{5}(4\sqrt{3}+2)$. It is reasonable to choose σ/a between 1 and $\sqrt{2}$. The repulsive part of the interatomic potential, which is expressed as the value at $r/a=1$ in our model, can be considered to be a measure of the softness of the interaction. For the same value of σ , the value of the Lennard-Jones potential at $r/a=1$ is extremely large as compared with that for the exponential-type potential.

At first, the system with the Lennard-Jones potential is considered. For several values of σ , this system is numerically investigated and it became clear that the system does not show the phase transition between the bcc solid and fcc solid. The only possible phase transition is the one between the fcc solid and fluid for any value of σ/a larger than 1. In Fig. 4, T - P phase diagrams for $\sigma/a = \frac{1}{2}(1+\sqrt{2})$ and $\sigma/a = \frac{1}{4}(3+\sqrt{2})$ are shown. The values of the potential at $r/a=1$ are 25.9085ϵ and 5.8244ϵ , respectively, and these are still very large compared with the value for the exponential-type potential with $\sigma/a = \frac{1}{5}(4+\sqrt{2})$ in Fig. 3. As far as the value of the potential at $r/a=1$ is finite, our

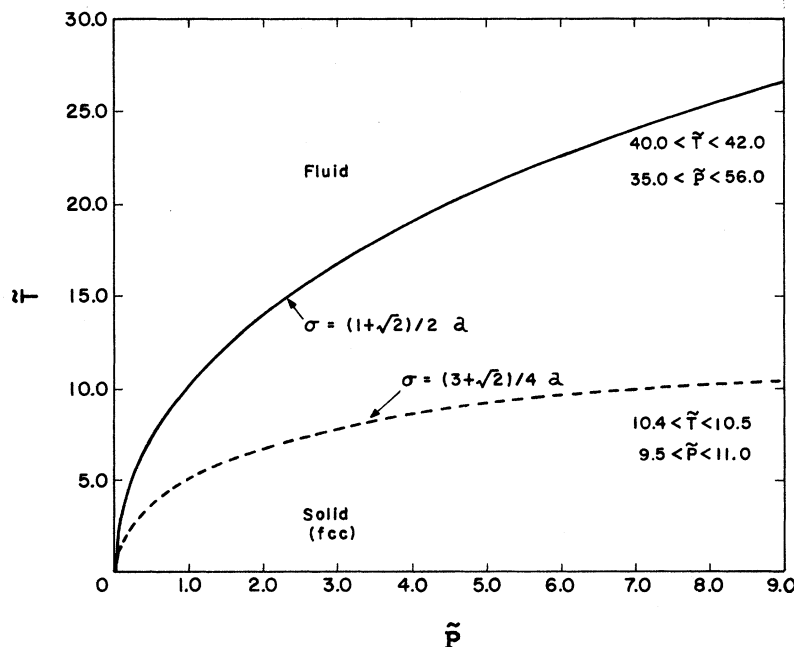


FIG. 4. T - P phase diagram for the system with the Lennard-Jones potential. Maximum point of the melting curves is approximately shown by inequality.

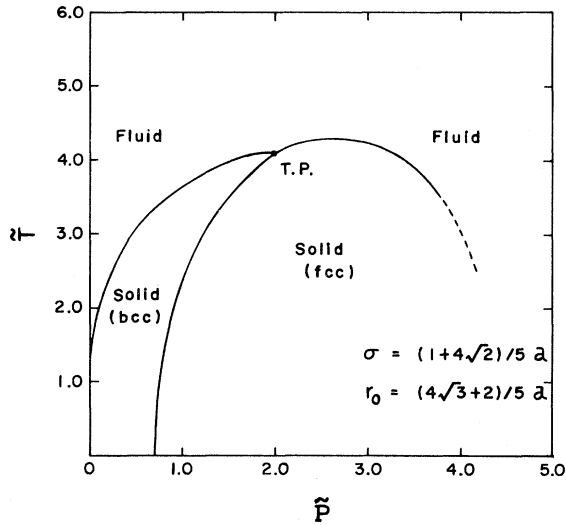


FIG. 5. T - P phase diagram for the system with the exponential type potential. The triple point is denoted by T. P.

system is expected to give rise to the high-pressure remelting. In fact, even the system with the Lennard-Jones potential shows the high-pressure remelting at an extremely high pressure in comparison with the pressure at which the system with the exponential-type potential remelts at the same temperature.

We shall consider the reason why the system described by the Lennard-Jones potential has only one solid phase of which lattice structure is fcc. The ordering energy is given by coefficient of R_b^2 or R_f^2 in the second term of Eq. (2.11) or (2.12):

$$E_b^{\text{order}} = -\frac{1}{3}[\phi(r_1) + 2\phi(r_2) - 4\phi(r_3) - 3\phi(r_4)](1 - \rho)^2, \quad (3.7)$$

$$E_f^{\text{order}} = -[3\phi(r_1) - 6\phi(r_2) + 4\phi(r_3) - 3\phi(r_4)](1 - \rho)^2. \quad (3.8)$$

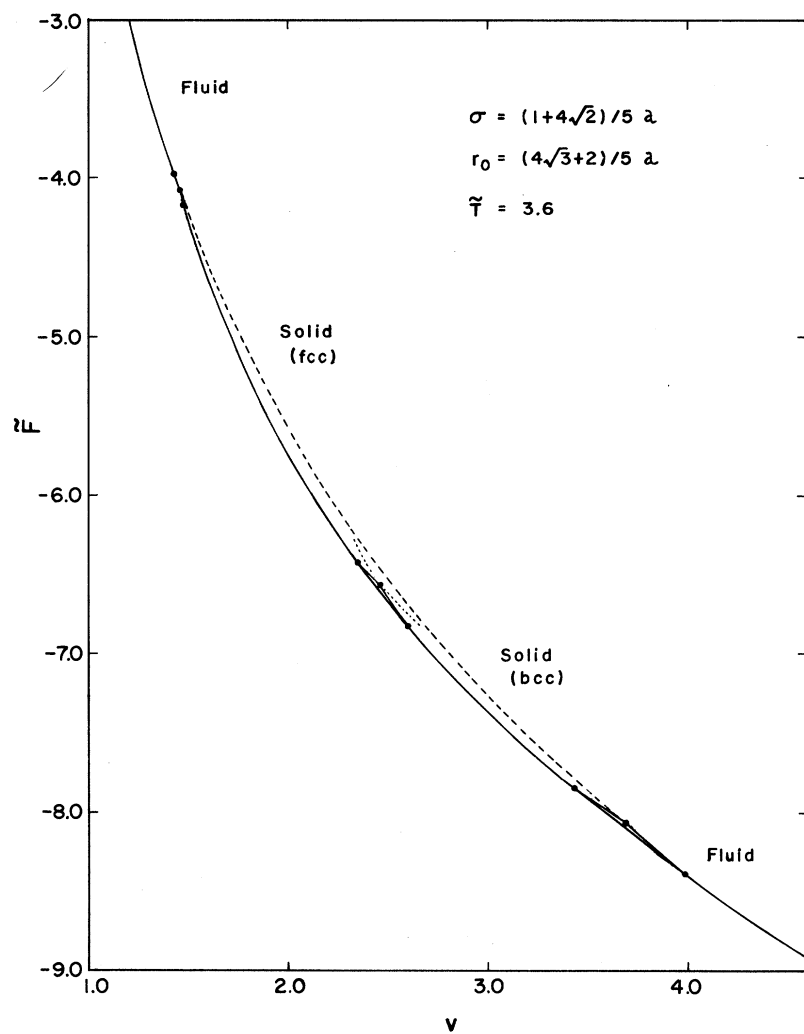
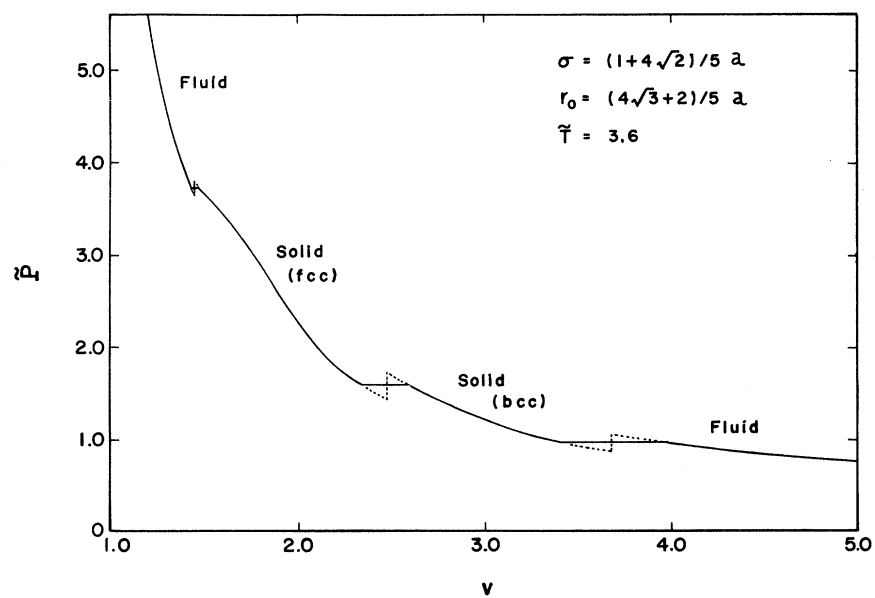
For σ/a not close to 1, $\phi(r_1)$ is sufficiently large that the dominant contribution to the ordering energy comes only from $\phi(r_1)$. Although both of the ordering energies are negative, the magnitude of the ordering energy for the fcc lattice structure is nine times as large as that for the bcc lattice structure. This means that the fcc lattice structure is stable as the solid phase. For σ/a close to 1, $\phi(r_1)$ does not give the dominant contribution to the ordering energy. In this case the distance at which the potential has its minimum value is between 1 and $\sqrt{2}$. The Lennard-Jones potential decays fast to zero as the function of distance. From these facts, the dominant contribution to the ordering energy seems to come from $\phi(r_2)$. The contribution from $\phi(r_2)$ to E_b^{order} is positive, but the one to E_f^{order} is negative. Even though the contributions from

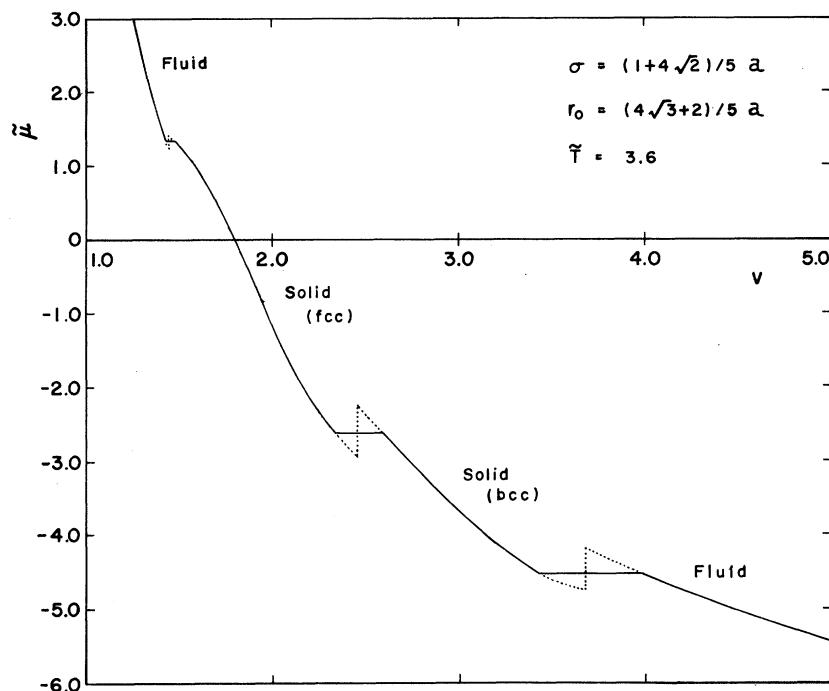
$\phi(r_1)$ and $\phi(r_3)$ are taken into account, the ordering energy for the fcc lattice structure is more negative than the one for the bcc lattice structure. Thus the system with the Lennard-Jones potential for σ/a larger than 1 always has the fcc lattice structure as the solid phase.

Next, we shall investigate the system in which the potential is given by Eq. (3.2). In Fig. 5, the temperature-versus-pressure phase diagram is shown for the case of $\sigma/a = \frac{1}{5}(1 + 4\sqrt{2})$ and $r_0/a = \frac{1}{5}(4\sqrt{3} + 2)$. Three phase transitions between the bcc solid and fcc solid, the bcc solid and fluid, and the fcc solid and fluid are obtained. It is rather natural to expect that the bcc solid phase is stable in the lower-pressure region and the fcc solid phase is stable in the higher-pressure region. The exponential-type potential gives rise to such a behavior as is shown in the diagram. Our attention is focused on the region near the triple point like the one in the first transition in the phase diagram of Cs. As compared with the melting curve of cesium in Fig. 1, the melting curve maximum for the bcc solid phase is not obtained, but the one for the fcc solid phase is. The slope of the transition line between the bcc solid and fcc solid is gently curved in our calculation. The isotherms for the free energy, pressure, and chemical potential versus volume are given in Figs. 6–8 at $\tilde{T} = 3.6$. The three phase transitions, which are between the bcc solid and fcc solid, the bcc solid and fluid, and the fcc solid and fluid are always accompanied by volume changes, and hence these are first-order phase transitions.

In order to investigate the effect of the softness of the interatomic potential upon the solid-solid phase transition, the value of the potential given by Eq. (3.2) at $r/a = 1$ is successively doubled, tripled, and quadrupled for fixed values of $\sigma/a = \frac{1}{5}(1 + 4\sqrt{2})$ and $r_0/a = \frac{1}{5}(4\sqrt{3} + 2)$ and the systems with these potentials are studied. As the value of the potential at $r/a = 1$ increases, the bcc solid phase shrinks down under the fcc solid phase in the phase diagram and the fcc lattice structure is more favored as the solid state. This situation is easily understood by recalling the discussion above of the Lennard-Jones potential. If the value of the potential $r/a = 1$ decreases, the bcc lattice structure becomes more favorable because the contribution from $\phi(r_3)$ to the ordering energy becomes dominant. But the melting curve in the high-pressure and low-temperature region has a positive value for $(\partial T/\partial P)_v$ after passing the maximum temperature.

The position where the potential is minimum is also important for obtaining the solid-solid phase transition. In both Figs. 2(a) and 2(b), the first-neighbor site is a β site and the fourth-neighbor site is an α site. The third-neighbor site in Fig. 2(a) and the second-neighbor site in Fig. 2(b) are α sites. Thus, when $\phi(r_1)$ does not have a dominant

FIG. 6. F - v curve at $\tilde{T}=3.6$.FIG. 7. P - v curve at $\tilde{T}=3.6$.

FIG. 8. μ - v curve at $\bar{T}=3.6$.

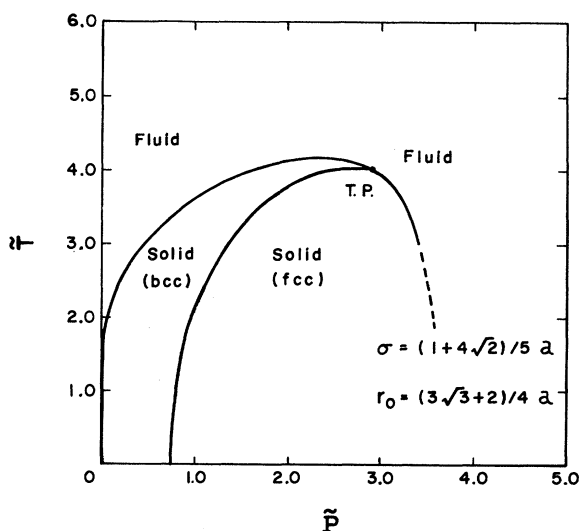
contribution to the ordering energy, $\phi(r_2)$ and $\phi(r_3)$ play an important role. If r_0/a is larger than $\frac{1}{5}(4\sqrt{3}+2)$, the bcc solid phase becomes stable up to the higher-pressure region. But if r_0/a is smaller than $\sqrt{3}$, the fcc solid phase becomes stable up to the lower-pressure region. In Fig. 9, T - P phase diagram is shown for $\sigma/a = \frac{1}{5}(1+4\sqrt{2})$ and $r_0/a = \frac{1}{4}(3\sqrt{3}+2)$.

IV. CONCLUDING REMARKS

By means of the classical lattice model, the phase transitions between the bcc solid and fcc solid, the bcc solid and fluid, and the fcc solid and fluid are obtained for the system described by the exponential type potential in the Bragg-Williams approximation. In our lattice model, the softness of the repulsive part of the interatomic potential as well as the distance at which the potential has its minimum value are important factors for the system to have the solid-solid phase transition. The system with the Lennard-Jones potential does not show the solid-solid phase transition and its solid structure is fcc. The result is consistent with the fact that the compressed rare gas, if it is described by the Lennard-Jones potential, has fcc lattice structure in the solid phase.

However, our theory still has many aspects which should be improved: The rigid-lattice model is used in our calculation. When the substance is compressed, it is reasonable to think that the lattice constant adjusts itself to the applied pressure. Recently, following LJD theory, in which the lattice

constant is changeable as a function of density, Yoshida and Okamoto⁴ discussed the high-pressure remelting for the system with potential $\phi(r) = \epsilon e^{-r/r_0}$. Mori *et al.*¹⁶ discussed the phase transition between the liquid and solid phases for a system with Lennard-Jones potential by using the expandable lattice model originally used by Peek and Hill,² in which the free energy is minimized with respect to a lattice expansion parameter. It is

FIG. 9. T - P phase diagram for the system with the exponential-type potential. The triple point is denoted by T.P.

hoped that the solid-solid and solid-fluid phase transitions may be investigated by using these expandable lattice models.

As for the statistical approximation used in our theory, it is the crudest one, that is, the Bragg-Williams approximation. Therefore, the short-range-order effects are completely ignored, in spite of their importance in the region of the solid state near the melting temperature, as well as in the fluid state. In order to take these effects into account, the pair approximation, which is equivalent to the Bethe approximation, the triangular approximation, etc., in the cluster-variation method¹⁷ will be used in the future.

As mentioned in Sec. I, in real systems like Cs, the interatomic distance does not change appreciably on phase transition from the bcc to fcc structures, while in the present theory it changes from $\sqrt{3}$ to $\sqrt{2}$ in units of the simple cube-edge length. To eliminate this drawback of the present formulation, the following improvement of the lattice model is suggested: Divide our original simple cubic lattice into a finer simple cubic lattice with lattice constant one-twentieth of the original value. Place the nearest-neighbor body-center lattice site at the fourth-neighbor distance along the body-diagonal direction and place the nearest-neighbor face-center lattice site at the fifth-neighbor distance along

the face-diagonal direction. The interatomic distance, in the solid phase in this improved lattice model will be $\sqrt{48}$ and $\sqrt{50}$ along the body-diagonal and face-diagonal directions, respectively. The number of β sites in this lattice will be substantially increased and average density will correspondingly be reduced. As long as the Bragg-Williams approximation is concerned, the elaboration of the theory to this model is straightforward, although lengthy.

Since the interatomic potential was originally determined experimentally by means of the second virial coefficient in the gas phase, whether the same potential can be used in dense phases is questionable. In addition, the potential in the solid phase may be different from the one in the fluid phase. In spite of these complications related to the nature of interatomic potential in condensed phases, the major mechanism of structural transition should be accounted for by statistical effects. The formulation discussed in this paper should offer an explanation in this direction.

ACKNOWLEDGMENTS

One of the authors (T. T.) is very grateful to Professor J. T. Shipman for the constant encouragement and the hospitality extended to him during his stay at Ohio University.

*On leave from The Catholic University of America.

¹J. E. Lennard-Jones and A. F. Devonshire, Proc. R. Soc. A **169**, 317 (1939); Proc. R. Soc. A **170**, 464 (1939).

²H. M. Peek and T. L. Hill, J. Chem. Phys. **18**, 1252 (1950).

³T. Morita, J. Phys. Soc. Jap. **14**, 572 (1959).

⁴T. Yoshida and H. Okamoto, Prog. Theor. Phys. **45**, 663 (1971).

⁵F. P. Bundy, Phys. Rev. **115**, 274 (1959).

⁶G. C. Kennedy, A. Jayaraman, and R. C. Newton, Phys. Rev. **126**, 1363 (1962).

⁷A. Jayaraman, Phys. Rev. **137**, A179 (1965).

⁸A. Jayaraman, R. C. Newton, and J. M. McDonough, Phys. Rev. **159**, 527 (1967).

⁹F. X. Kayser, Phys. Rev. Lett. **25**, 662 (1970).

¹⁰N. Kawai and Y. Inokuti, Jap. J. Appl. Phys. **7**, 989 (1968); Jap. J. Appl. Phys. **9**, 31 (1970).

¹¹J. Bardeen, J. Chem. Phys. **6**, 372 (1938).

¹²Referred to by R. Sternheimer [Phys. Rev. **78**, 235 (1950)].

¹³R. Ramirez and L. M. Falicov, Phys. Rev. B **3**, 2425 (1971).

¹⁴Y. Kuramoto and H. Furukawa, Prog. Theor. Phys. **47**, 1069 (1972).

¹⁵T. Morita and T. Tanaka, Phys. Rev. **145**, 288 (1966).

¹⁶H. Mori, H. Okamoto, and S. Isa, Prog. Theor. Phys. **47**, 1087 (1972).

¹⁷T. Morita, J. Math. Phys. **13**, 115 (1972).